3D Finite Element Modeling of Embankments on Soft Soil Deposits Improved by Preloading Accompanied by PVDs

Mahmoud S. Hammad[1], Ayman L. Fayed[2], Yasser M. El-Mosallamy[3]

[1, 2, 3]Ain Shams University, Faculty of Engineering, Structural Department, 1 Elsarayat St., Abbaseya, 11517 Cairo, Egypt

Abstract: ***Three-dimensional finite element analysis was utilized to investigate the application of preloading technique with the presence of PVDs as a method to improve soft soil deposits under embankments. Back analyses of two embankments with and without PVD were performed using PLAXIS 3D 2018. The behavior of soft soil deposits was modeled using soft soil creep model (SSC) during the back analyses. The back analyses showed very good agreement between the F.E. model and the field measurements. Also, the soft soil model (SS) and hardening soil model (HS) were utilized and compared to the behavior of the (SSC) models. The comparison showed that both models predict less settlement than the (SSC) model as they do not take the creep of the soft soil deposits into consideration, however, they can be accurately used if the predicted creep is negligible.***

Keywords: Soft soil, Soil improvement, Preloading, PVDs, Vertical Drains.

1. Introduction

Soft soils are usually located near most river estuaries and coastal areas all over the world. In Egypt, the soft soil deposits are most commonly found near its northeastern coast in Port Said and Damietta where major development planes are currently undertaken. Most structures built on these deposits are incompatible with such weak foundation soil conditions.

The preloading technique is one of the most applied soil improvement techniques due to its simplicity, reliability, as well as its economic aspects, compared to other techniques.

The simplest method of preloading is by means of an embankment. When the load is placed on the soft soil, it is initially carried by the pore water. When the soil has very low permeability, which is normally the case, the water pressure will decrease gradually because the pore water is only able to dissipate very slowly in the vertical direction only. In order not to create any stability problems, the load must mostly be placed in two or more stages. After the settlement exceeds the predicted final settlement of the required structure the applied temporary surcharge can be removed. It is preferable that the surcharge is not removed until the remaining excess pore pressure is below the stress increase caused by the temporary surcharge. Furthermore, the secondary settlement can be reduced or even eliminated by increasing the time of temporary overloading or the size of the overload. This is contributed to the fact that by using a surcharge higher than the workload causes the soil to in an over consolidated state and the secondary compression for over consolidated soil is much smaller than that of normally consolidated soil, which will benefit greatly the subsequent geotechnical design [1].

A major disadvantage of the conventional preloading technique is the very long time required to reach the needed consolidation, even with the application of very high surcharge load, especially in soft soil deposits as they are usually characterized by very low permeability, thus, the application of preloading alone may not be feasible with tight construction schedules. Several techniques can be adopted to accelerate the preloading process, such as vacuum preloading or introducing a system of vertical drains.

Since the 1970s, preloading accompanied by vertical drains has been used extensively as an improvement technique for soft soil deposits. The vertical drains were used as a means of accelerating the consolidation process, due to the preload, by supplying additional routes for the excess pore water pressure to dissipate via radial drainage, thus, accelerating the preloading process.

2. Case study - Changi East reclamation Project

2.1 Introduction to Changi East

The case study adopted during the research lies within the Changi East reclamation project located in the Republic of Singapore. The Changi East site offers continuous land reclamation and ground improvement works in order to keep up with the continuous expansion of the Changi International Airport. The location and layout of the Changi East reclamation project are shown in Figure 1. The original site is completely submerged underwater with sea bed elevation laying 4 to 10 meters below average sea level.

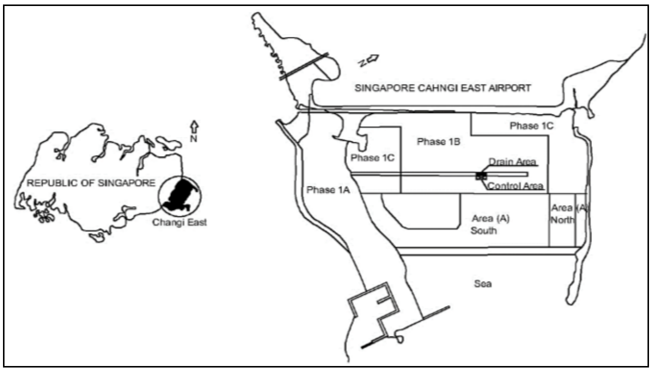

Figure 1: Location and Layout of Changi East project **[2]**

The preliminary description and the determination of the characteristics of the soil layers within the Changi East area was possible by means of extensive soil investigation works. The soil investigations indicated the presence of three distinct soil layers, an upper marine clay layer with depth up to 35 meters below average sea level, followed by an intermediate stiff clay layer with thickness ranging between 3 to 5 meters, finally, a lower marine clay layer extending up to 60 meters below average sea level. Both the upper and lower marine clay layers can be considered high to very high plastic silty clay layers, however, the upper clay layer was found to be more compressible than the lower clay layer [3] and [4]. The range of parameters for the various soil layers as stated in Table 1.

Table 1: Ranges for various soil parameters at Changi East [**3**]

Parameters	Upper Marine Clay	Intermediate Marine Clay	Lower Marine Clay
γ_{bulk} (kN/m3)	14.23-15.7	18.64-19.6	15.7-16.67
WC (%)	70-88	10-35	40-60
LL (%)	80-95	50	65-90
PL (%)	20-28	18-20	20-30
e_o	1.8-2.2	0.7-0.9	1.1-1.5
G_s	2.6-2.72	2.68-2.76	2.7-2.75
c_c	0.6-1.5	0.2-0.3	0.6-1.0
c_α	0.012-0.025	0.0043-0.023	0.012-0.023
c_r	0.09-0.16	0.08-0.15	0.14-0.2
c_v (m^2/year)	0.47-0.6	1-4.5	0.8-1.5
c_{vr} (m^2/year)	3-7	10-30	4-10
c_h (m^2/year)	2-3	5-10	3-5
OCR	1.5-2.5	3-4	2

2.2 Description of the case study

The presented case study lies within the northern area of the site where the new airport runway is now located. The northern area of the site is characterized by the presence of soft marine clay layers reaching to a depth of 35.5 meters below average sea level, while the sea bed lies about 5.5 meters below sea level. The case study consists of two adjacent embankments with the height of both embankments reaching 8 meters above average sea level. The embankment where PVDs are installed, where the runway is now located, is referred to as the main embankment where vertical drains are installed. While the second embankment is referred to as the control area at which no vertical drains were used. The location of the two embankments can be shown in Figure 1.

The two embankments were constructed together with the same construction sequence and surcharge heights to be able to compare the behavior of both. Land reclamation works were performed by hydraulic placement of sand until 2 meters above sea level was reached. The vertical drains were then installed, in the vertical drain area only, from this elevation to a depth of 35.5 meters below sea level. Soil instrumentations were installed directly before the installation of the PVDs in both the drain and control areas. Reclamation sand was then used to apply the surcharge load by completing the construction of both embankments until a final height of 8 meters above sea level is reached. The construction sequence of the embankments at the main embankment and the control embankment are shown in Figure 2 and Figure 3 respectively.

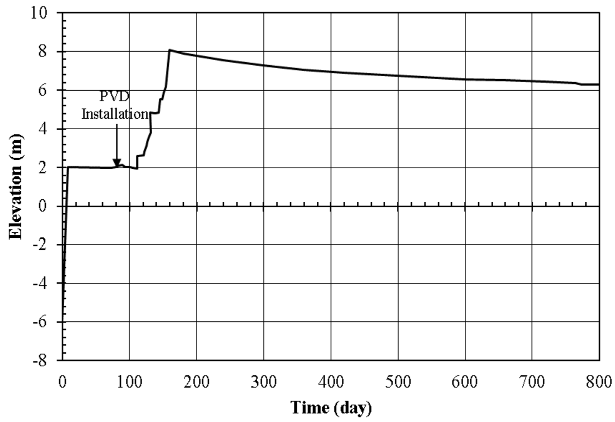

Figure 2: Construction sequence for the main embankment **[2]**

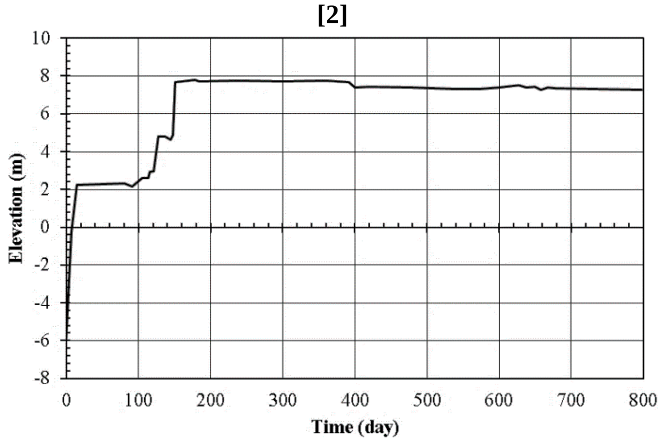

Figure 3: Construction sequence for the control embankment [**2**]

Two types of PVDs were used in the project, Colbond CX1000 and Mebra MD7007. The specifications for the used PVDs are described in

Table 2 [5]. The PVDs were installed in a square pattern with a 1.5 meter spacing between them and extended throughout the entire depth of the compressible soil layers.

Table 2: Specifications of used PVDs [5]

Parameter	*Width*	*Thick.*	*Discharge capacity (at 350 kPa)*		*Pore size (O95)*	*Permittivity*
			Straight	*Buckled*		
	(mm)	(mm)	10-6 m3/sec		µm	s-1
Value	100	3-4	>25	>10	<75	>0.005

Instrumentations were used to monitor the behavior of both embankments during and after applying the surcharge load. Surface settlement plates, deep settlement gauges were used to monitor the vertical deformation of soil at several depths, Also Pneumatic, electric and open type piezometers were used to measure the pore water pressure at various depths. The levels of various instrumentations installed under both the main and control embankments are shown in Figure 4.

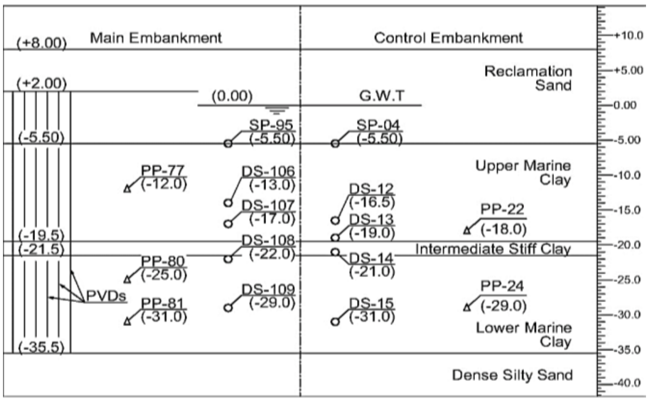

Figure 4: Instrumentations under main and control embankments [2]

As shown in Figure 5 and Figure 6 respectively, Settlement and pore water pressure readings were recorded under main embankments at various depths using the previously described instrumentations. Similar field measurements recorded for the control embankment are shown in Figure 7 and Figure 8. The readings were recorded periodically over a period of about 23 months after the PVD installation or a total period of about 26 months.

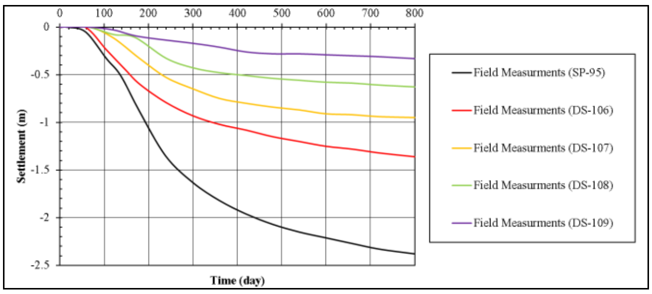

Figure 5: Field settlement under main embankment [2]

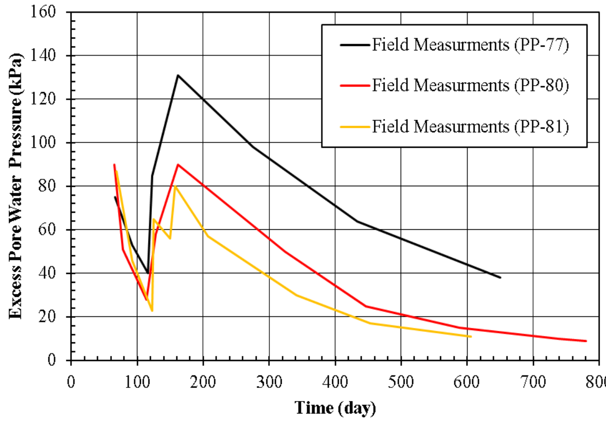

Figure 6 Field excess pore water pressure under the main embankment [2]

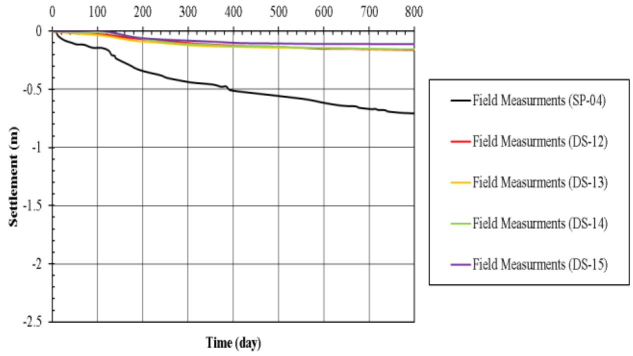

Figure 7: Field settlement under control embankment [2]

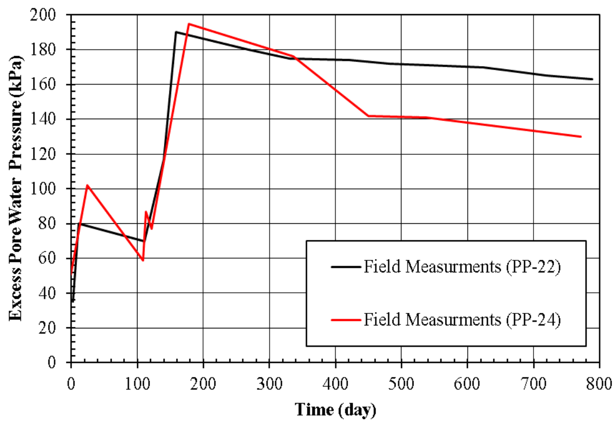

Figure 8: Field excess pore water pressure under control embankment [2]

3. Back analyses of the Case Study

The back analysis of the case study is performed using a three-dimensional finite element model. The model is built using the finite element code PLAXIS 3D 2018. The performed study includes the back analysis of two embankments, the control embankment where no PVDs were installed, and the main embankment where PVDs are used. The back analyses are based on the settlement and pore water pressure readings previously shown.

First, the back analysis of the control embankment is performed to verify the chosen constitutive laws and soil parameters without taking the various effects of the installation and buckling of the PVDs into account. After the chosen constitutive laws, soil parameters, model geometry, and boundaries are verified, the back analysis of the main embankment is then performed.

3.1 Back analysis of the control embankment

During the back analysis of the control embankment, Soft soil creep (SSC) model is chosen to model the upper marine, intermediate stiff and lower marine clay layers respectively. The main advantage of the (SSC) model is that it accurately depicts the behavior of soft soil deposits while taking the secondary consolidation, i.e. creep, into consideration. The effective strength parameters in undrained conditions are used for the clay layers. The reclamation sand is modeled using the Mohr-Coulomb (MC) model and the drained soil condition. The soil parameters used to model various soil layers are shown in **Error! Reference source not found.**.

Table 3: Soil parameters used in the back analysis of the control embankment

Parameters	*Upper Marine Clay*	*Intermediate Stiff Clay*	*Lower Marine Clay*	*Reclamation Sand*
Constitutive Model Type	SSC	SSC	SSC	MC
Drainage Condition	Undrained	Undrained	Undrained	Drained
$\gamma_{unsat.}$ *(kN/m³)*	15	19	15	17
$\gamma_{sat.}$ *(kN/m³)*	15.5	19.5	16	20
k_x, k_y *(m/sec)*	10.2 $x10^{-10}$	13.8 $x10^{-10}$	9.96 $x10^{-10}$	1
k_z *(m/sec)*	5.1 $x10^{-10}$	6.94 $x10^{-10}$	4.98 $x10^{-10}$	1
c_k	1.1	0.35	0.75	1 $x10^{15}$
c'_{ref} *(kN)*	1	1	1	1
φ' *(o)*	27	32	27	31
ψ' *(o)*	0	0	0	0
e_o	2.2	0.7	1.5	0.5
λ^*	0.095	0.077	0.104	-------
κ^*	0.027	0.072	0.049	-------
μ^*	0.163 $x10^{-2}$	0.059 $x10^{-2}$	0.209 $x10^{-2}$	-------
OCR	2.5	3	2	-------
E' (kN/m²)	-------	-------	-------	13000
E_{oed} *(kN/m²)*	-------	-------	-------	17500
G (kN/m²)	-------	-------	-------	5000
ν'	-------	-------	-------	0.3

As the embankment lies over a large area, modeling the entire embankment is inconvenient. Thus, a portion of the embankment only is modeled and used to represent the entire control embankment. Since the PVDs installed in the main embankments have a square pattern with spacings of 1.5 meters in both directions, the horizontal extents of the model are chosen to be 4.5 meters in both X and Y directions to allow for the modeling of 3 rows and 3 columns of the PVDs. According to the soil profile shown in Figure 4 the lower horizontal boundary of the model is chosen at the end of the lower marine clay layer at Z=-33.5.

The horizontal movement only was restricted at all vertical boundaries, while both horizontal and vertical movements were not allowed at the lower boundary of the model. Furthermore, while the drainage of the pore water is allowed in order to take the presence of a highly permeable layer of stiff silty sand below the lower marine clay layer into consideration, the drainage through all vertical boundaries is prevented. The model shape, geometry, and meshing are shown in Figure 9.

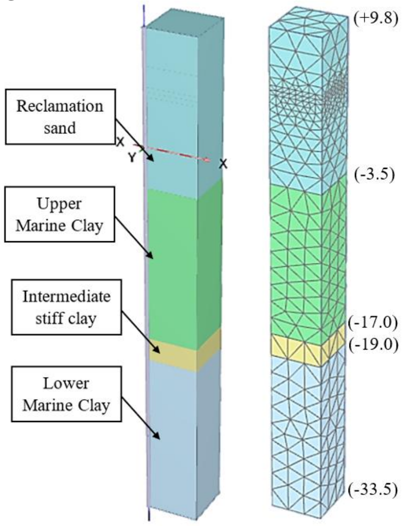

Figure 9: Developed finite element mesh for the control embankment

As shown in Figure 8, An idealized construction sequence with very slight variations from the actual sequence is adopted during the numerical modeling.

The comparison between field settlement measurements and settlement calculated by the F.E. model at various depths below the control embankment shows a very good agreement. As shown in Figure 11, The settlement predicted by the 3D F.E. model at various depths are found to be slightly higher than the actual settlement readings during the first 150 days, i.e. the construction period, which can return to the slight variations between the actual construction procedure and the construction sequence adopted during the numerical modeling, after which, the behavior of the numerical model almost coincide with the field measurements.

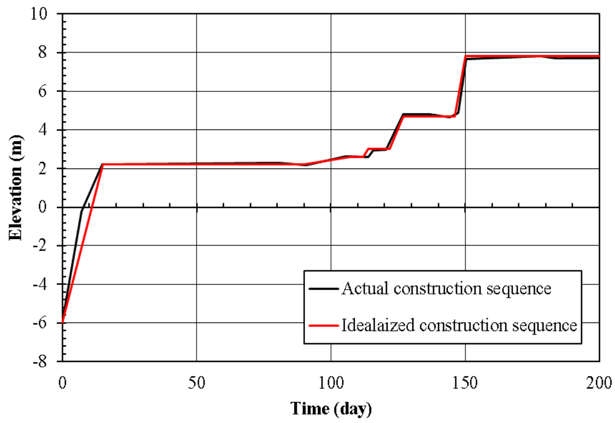

Figure 10: Comparison between actual and idealized construction sequence of control embankment

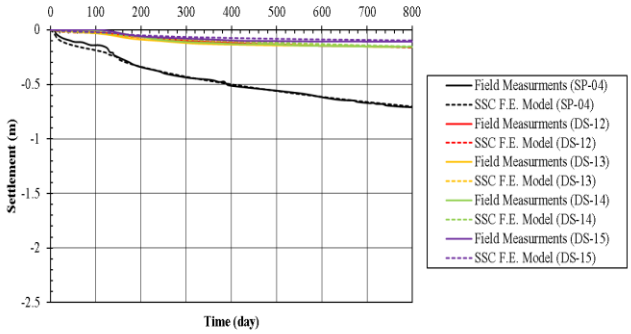

Figure 11: Comparison between field measurements for settlement and results of the F.E. model for control embankment

The excess pore water pressure predicted by the numerical model shows good agreement with the field measurements at various piezometers, as the peak excess pore water pressure calculated by the F.E. model coincides with the peak excess pore water pressure measured at the site.

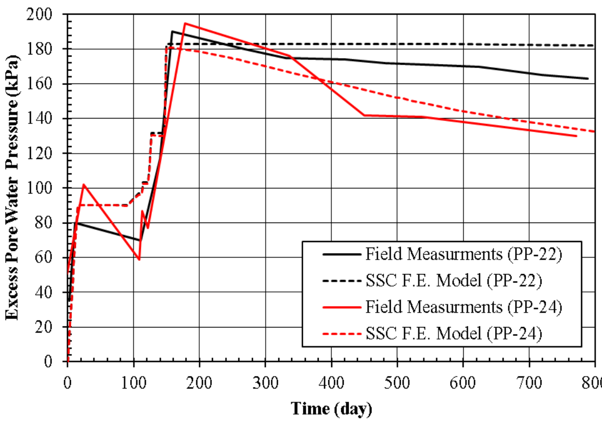

Figure 12: Comparison between Field measurements of excess pore water pressure and results of F.E. model for control embankment

3.2 Back analysis of the main embankment

The constitutive models used for the back analysis of the main embankment are the same used during modeling of the control embankment. Furthermore, the soil parameters used in modeling of the main embankment are shown in Table 4.

Table 4: Soil parameters used in the back analysis of the main embankment

	Parameters	*Upper Marine Clay*	*Intermediate Stiff Clay*	*Lower Marine Clay*	*Reclamation Sand*
	Constitutive Model Type	SSC	SSC	SSC	MC
	Drainage Condition	Undrained	Undrained	Undrained	Drained
	$\gamma_{unsat.}$ *(kN/m³)*	15	19	15	17
	$\gamma_{sat.}$ *(kN/m³)*	15.5	19.5	16	20
Before PVD installation	k_x, k_y *(m/sec)*	10.2 x10^{-10}	13.8 x10^{-10}	9.96 x10^{-10}	1
Before PVD installation	k_z *(m/sec)*	5.1 x10^{-10}	6.94 x10^{10}	4.98 x10^{-10}	1
	k_x, k_y *(m/sec)*	5.1 x10^{-10}	6.94 x10^{-10}	4.98 x10^{-10}	1
	k_z *(m/sec)*	2.55 x10^{-10}	3.47 x10^{-10}	2.49 x10^{-10}	1
	c_k	1.1	0.35	0.75	1 x10^{15}
	c'_{ref} *(kN)*	1	1	1	1
	φ' *(o)*	27	32	27	31
	ψ' *(o)*	0	0	0	0
	e_o	2.2	0.7	1.5	0.5
	λ^*	0.095	0.077	0.104	-------
	κ^*	0.027	0.072	0.049	-------
	μ^*	0.163 x10^{-2}	0.059 x10^{-2}	0.209 x10^{-2}	-------
	OCR	2.5	3	2	-------
	E' (kN/m²)	-------	-------	-------	13000
	E_{oed} *(kN/m²)*	-------	-------	-------	17500
	G (kN/m²)	-------	-------	-------	5000
	ν'	-------	-------	-------	0.3

The adopted reduction in soil permeability was introduced by Lin et al. (2000) [6] as a method to represent the disturbance occurring in the soil layer within the smear zone due to the installation of the PVD. Ideally, the soil surrounding the vertical drains should be modeled as two different soil clusters, the undisturbed soil mass where the soil parameters are the same as the original soil, and the smeared soil cluster in direct proximity with the PVD having much lower permeability than the undisturbed soil. However, modeling the smear zone as a different soil cluster was found to be inconvenient during the 3D F.E. modeling as it causes several errors to occur during meshing. Thus, the soil mass surrounding the PVD is modeled as one soil cluster having all soil parameters as the undisturbed soil, but with a lower equivalent permeability calculated by Equation 1

$$k_e = \frac{k_h \ln(\frac{r_e}{r_w})}{\ln(\frac{r_e}{r_s}) + \frac{k_h}{k_{se}} \ln(\frac{r_s}{r_w})} \qquad \text{Equation 1}$$

Where, (r_e) is the radius of the influence zone, (r_w) is the equivalent radius of the drain, (r_s) is the radius of the smear zone, (k_s) is the soil permeability within the smear zone, (k_e) is the soil equivalent soil permeability.

For soft Bangkok clay, Bergado et al. (1992) [7] has verified the diameter of the smear zone to range between two to three times the equivalent cross-sectional area of the mandrel, furthermore, the permeability within the smear zone was found to be in the range of 0.33 to 0.5 that of the undisturbed soil. Thus, the permeability of the equivalent soil used in numerical modeling shall be about 50% of the permeability of the undisturbed soil.

Same geometry of the model and same boundary conditions discussed during the back analysis of the control embankment are applied. Additionally, nine PVDs with 1.5 meters spacing in X and Y directions are modeled as vertical drains. The drains are activated in the model only by the time their installation was finished in the field (t ≈ 80 days). The generated meshes for the finite element model are shown in Figure 13. Furthermore, the comparison between actual and idealized construction sequences adopted during the back analysis is shown in Figure 14.

International Journal of Science and Research (IJSR)
ISSN: 2319-7064
ResearchGate Impact Factor (2018): 0.28 | SJIF (2018): 7.426

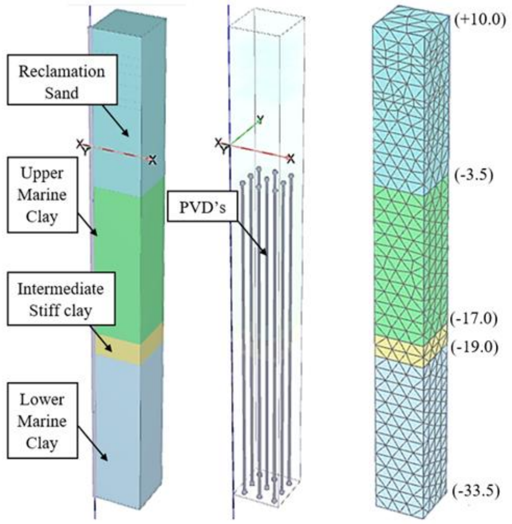

Figure 13: Developed finite element mesh for the main embankment

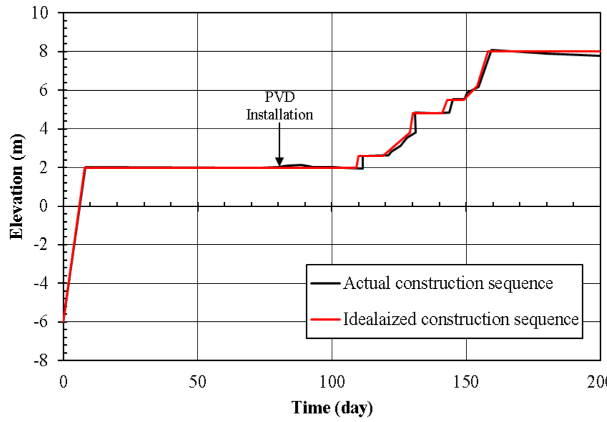

Figure 14: Comparison between actual and idealized construction sequence of the main embankment

Figure 15 indicates good agreement between the settlement results yielding from the F.E. model and the field measurements taken at various settlement gauges. The results of the numerical model are slightly higher than the field measurements until we reach the 400-day mark. This is due to the slight alteration of the construction sequence used in the numerical modeling from the actual construction sequence. After 400 days, the results of the numerical model align with the field measurements until the end of the field readings at 800 days.

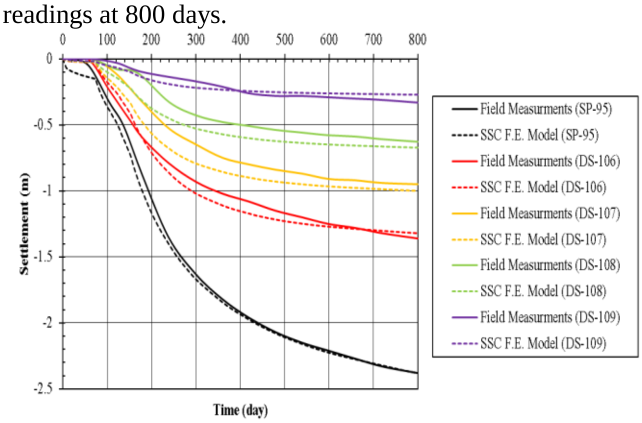

Figure 15: Comparison between field measurements for settlement and results of the F.E. model for the main embankment

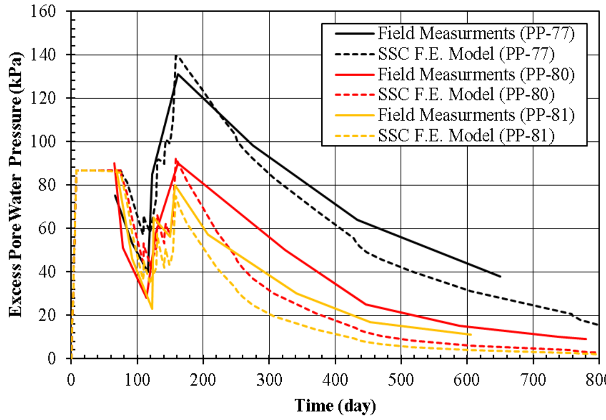

Figure 16: Comparison between Field measurements of excess pore water pressure and results of F.E. model for the main embankment

Furthermore, although the comparison between the excess pore water pressure calculated from the F.E. model and that measured at the site is accepted, Figure 16 shows that the rate of dissipation of the excess pore water pressure at the site is lower than that yielding from the F.E. model. This can return to the slight disturbance of the soil surrounding the piezometers due to their installation which can, in turn, affect the field measurements.

4. Numerical modeling using different Constitutive Models

To further study the numerical analysis of the PVDs, the case study is reinvestigated using the Soft Soil model (SS) and the hardening soil model (HS) to represent the clay layers instead of the (SSC) model adopted during the back analyses. The new F.E. models respect the same geometry, boundary conditions, and construction sequence of the verified (SSC) model. Table 5 and Table 6 state the soil parameters used for the different soil layers in both the (SS) and (HS) models respectively.

A comparison between the settlement readings calculated using different soil models at (SP-04) under the control embankment is shown in Figure 17. The comparison shows that the results yielding from the (HS) model are slightly higher throughout the investigated time period. The (SS) model predicts higher settlement values than those calculated by the (SSC) model during the first 500 days after which it resides below the readings of the (SSC) model results until the 800-day mark. However, the difference between the three models did not exceed 3% at any given time.

Table 5: Soil parameters used for the Soft soil model (SS)

Parameters	*Upper Marine Clay*	*Intermediate Stiff Clay*	*Lower Marine Clay*	*Reclamation Sand*
Constitutive Model Type	SS	SS	SS	MC
Drainage Condition	Undrained	Undrained	Undrained	Drained
$\gamma_{unsat.}$ (kN/m^3)	15	19	15	17
$\gamma_{sat.}$ (kN/m^3)	15.5	19.5	16	20
PVI nst k_x, k_y	10.2	13.8	9.96	1

	(m/sec)	x10^{-10}	x10^{-10}	x10^{-10}	
	k_z *(m/sec)*	5.1 x10^{-10}	6.94 x10^{10}	4.98 x10^{-10}	1
After PVD installation	k_x, k_y *(m/sec)*	5.1 x10^{-10}	6.94 x10^{-10}	4.98 x10^{-10}	1
	k_z *(m/sec)*	2.55 x10^{-10}	3.47 x10^{-10}	2.49 x10^{-10}	1
c_k		1.1	0.35	0.75	1 x10^{15}
c'_{ref} *(kN)*		1	1	1	1
φ' *(o)*		27	32	27	31
ψ' *(o)*		0	0	0	0
e_o		2.2	0.7	1.5	0.5
λ^*		0.095	0.077	0.104	-------
κ^*		0.027	0.072	0.049	-------
OCR		2.5	3	2	-------
E' (kN/m²)		-------	-------	-------	13000
E_{oed} *(kN/m²)*		-------	-------	-------	17500
G (kN/m²)		-------	-------	-------	5000
v'		-------	-------	-------	0.3

Table 6: Soil parameters used for the hardening soil model (HS)

Parameters		*Upper Marine Clay*	*Intermediate Stiff Clay*	*Lower Marine Clay*	*Reclamation Sand*
Constitutive Model Type		HS	HS	HS	MC
Drainage Condition		Undrained	Undrained	Undrained	Drained
$\gamma_{unsat.}$ *(kN/m³)*		15	19	15	17
$\gamma_{sat.}$ *(kN/m³)*		15.5	19.5	16	20
Before PVD installation	k_x, k_y *(m/sec)*	10.2 x10^{-10}	13.8 x10^{-10}	9.96 x10^{-10}	1
	k_z *(m/sec)*	5.1 x10^{-10}	6.94 x10^{10}	4.98 x10^{-10}	1
After PVD installation	k_x, k_y *(m/sec)*	5.1 x10^{-10}	6.94 x10^{-10}	4.98 x10^{-10}	1
	k_z *(m/sec)*	2.55 x10^{-10}	3.47 x10^{-10}	2.49 x10^{-10}	1
c_k		1.1	0.35	0.75	1 x10^{15}
c'_{ref} *(kN)*		1	1	1	1
φ' *(o)*		27	32	27	31
ψ' *(o)*		0	0	0	0
E_{50} (kN/m²)		1320	1630	1200	-------
E_{oed} (kN/m²)		1050	1030	960	-------
E_{ur} (kN/m²)		6630	3260	3700	-------
OCR		2.5	3	2	-------
E' (kN/m²)		-------	-------	-------	13000
E_{oed} *(kN/m²)*		-------	-------	-------	17500
G (kN/m²)		-------	-------	-------	5000
v'		-------	-------	-------	0.3

Furthermore, as shown in Figure 18, the settlement at (SP-95) below the main embankment calculated by both the (HS) and (SS) models is slightly higher than the settlement readings predicted by the (SSC) for a short period after the embankment construction is finished. However, the settlement values yielding from both the (SS) and (HS) models start to be less than the settlement of the (SSC) model after the soft soil reaches a degree of consolidation of about 33% to 50% for the (SS) and (HS) models respectively. the reduction in the predicted settlement occurs as both (SS) and (HS) models do not take the secondary consolidation, i.e. creep, into consideration.

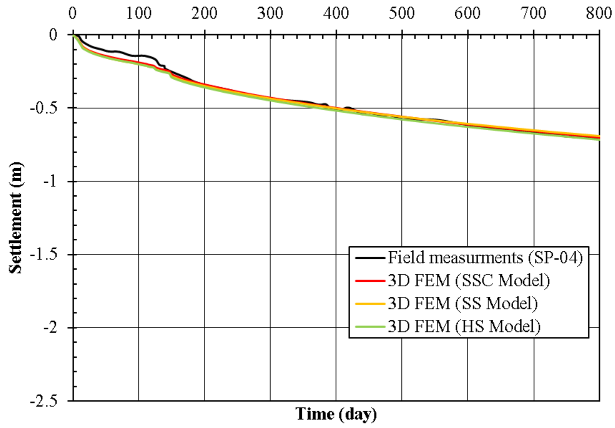

Figure 17: Comparison between results SSC, SS, and HS F.E. models and field measurements at (SP-04)

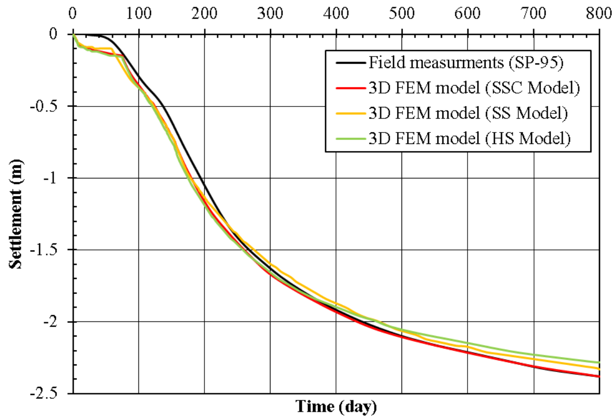

Figure 18: Comparison between results SSC, SS, and HS F.E. models and field measurements at (SP-95)

5. Summary and Conclusions

During this research, three-dimensional finite element analysis was utilized to investigate the application of preloading technique with the presence of PVDs as a method to improve soft soil deposits under embankments. Back analyses of two embankments with and without PVD were performed using PLAXIS 3D 2018. The behavior of soft soil deposits was modeled using soft soil creep model (SSC) during the back analyses. Also, the soft soil model (SS) and the hardening soil model (HS) were utilized and compared to the behavior of the (SSC) models. The research conclusions can be summarized as follows:

- Applying Three-dimensional finite element modeling can be used to simulate the improvement of soft soil deposits using the preloading technique with the presence of PVDs provided suitable geometry, boundary conditions and constitutive laws are used.
- The soft soil model (SS) and the hardening soil model (HS) predict less settlement than the soft soil creep model (SSC) as they do not take soil creep into consideration.
- (SS) and (HS) models can be used to accurately predict the behavior of soft soil layers with relatively small secondary consolidation compression index. However, (SSC) model

is preferable for all soft soil layers as it takes creep into consideration.

References

[1] J. Chu, M. Bo and V. Choa, "Practical considerations for using vertical drains in soil improvement projects," Geotextiles and geomembranes 22 (1-2), pp. 101,117, 2004.
[2] A. Arulrajah, Field measurements and back-analysis of marine clay geotechnical characteristics under reclamation fills, Western Australia: Curtin University of Technology - PhD Thesis, 2005.
[3] M. W. Bo, A. Arulrajah and V. Chao, "Hydraulic conductivity of Singapore marine clay," The quartarly journal of engineering geology, Vol. 31, Part 4, pp. 291-299, 1998.
[4] A. Arulrajah and M. W. Bo, "Reclamation at Changi East - Phase 1C Geotechnical Desing Report," Singapore, 1995.
[5] J. Chu, M. W. Bo and A. Arulrajah, "Soil improvement works for an offshore land reclamation," Geotechnical Engineering, Issue GE1, pp. 21-32, 2009.
[6] D. Lin, H. Kim and A. Balasubramaniam, "Numerical modelling of prefabricated vertical drains," Geotechnical Engineering Journal, Southeast Asian Geotechnical Society, Vol. (31), No. (2), pp. 109-125, 2000.
[7] D. Bergado, H. Asakami, M. Alfaro and A. Balasubramaniam, "Smear effects of vertical drains on soft Bangkok clay," Journal of Geotechnical Engineering, ASCE, Vol. (117), No. (10), pp. 1509-1530, 1991.

Author Profile

Mahmoud El Shawaf received the B.S. and M.S. degrees in Structural Engineering from Ain Shams University in 2008 and 2014, respectively. Since 2009, he works as a teaching assistant at the Faculty of Engineering of Ain Shams University to study and Geotechnical Engineering topics including soil mechanics and foundations with a special focus on behavior of soft soil deposits and soil improvement techniques.